

Multi-Channel Interference in High-Order Above-Threshold Ionization

Long Xu¹ and Libin Fu^{1,*}

¹*Graduate School of China Academy of Engineering Physics,
No. 10 Xibeiwang East Road, Haidian District, Beijing, 100193, China*

The intensity-dependent resonance-like enhancements phenomenon in high-order above-threshold ionization spectrum is a typical quantum effect for atoms or molecules in the intense laser field, which has not been well understood. The calculations of TDSE are in remarkable agreement with the experimental data, but it can not clarify the contributions of the bound states. The semi-classical approach of strong field approximation, in which no excited states are involved, can obtain the similar phenomenon, but the laser intensities of enhanced regions predicted by SFA are inconsistent with the results of TDSE. In this letter, a new full quantum model is established from TDSE with no any excited states. The theoretical calculations of this model agree well with the results of TDSE. Since there are no any excited states in the new model, the results verify the facts of SFA that excited states have little contribution to the resonance-like enhancements. We show that such resonance-like enhancements are caused by the constructive interference of different momentum transfer channels with the help of the combination of the laser field and the ionic potential. At last, the Fano-like lineshapes are also discussed for the features of multi-channel interference.

Above-threshold ionization (ATI) is the most fundamental and essential nonperturbative phenomenon in the interaction of the intense laser pulse with atoms or molecules, and it has attracted extensive attention [1–3] due to various possible applications since it was first observed forty years ago [4]. ATI reveals that the electron can absorb more photons than required to exceed the ionization threshold for atoms or molecules in the intense laser field. The ATI spectra have been well understood by combining the contributions of the direct ionization and the rescattering process. For the electron kinetic energy less than $2U_p$, the ATI spectrum decreases exponentially, where $2U_p$ is the maximal energy of a directly ionized electron [5–7], and $U_p = E_0^2/(4\omega^2)$ is the ponderomotive energy, E_0 and ω are the laser peak intensity and laser frequency, respectively. The high-energy spectrum appears a flat plateau extending to $10U_p$ [6–8], which is originated from the elastic scattering of electron when it revisits the parent ion.

In addition to the aforementioned features, an intensity dependent enhancements phenomenon in high-order ATI spectrum, the so-called resonance-like enhancements (RLEs) was discovered in the rare gases Xenon [9] and Argon [10] two decades ago, triggers great interest both experimentally and theoretically. In 2003, Grasbon *et al* [11] discovered that RLEs are pronounced in multi-cycle laser pulses and will be suppressed in few-cycle pulses. Recently, the RLEs were also observed experimentally in the molecular system including H_2 [12], N_2 [13], formic acid [14], the polyatomic molecules C_2H_4 and C_2H_6 [15]. RLEs are very sensitive to the laser intensity, and only a few percent increases in the laser intensity will result in the ATI peaks on the plateau enhanced by up to an order of magnitude. In the past two decades, great efforts have been made to study the underlying mechanism, but no consensus has yet been reached.

RLEs are indeed the quantum effects of atoms or

molecules in the intense laser field, and cannot be described by the classical (semiclassical) three-step model [8], although it has successfully explained the main features of ATI spectrum. The theoretical calculations of the time-dependent Schrödinger equation (TDSE) in the single active electron approximation are in remarkable agreement with the experimental data, indicating that high-order ATI can be explained by single electron dynamics [16]. The interpretations based on the results of TDSE [17–19] and the Floquet approach [19–22] suggest that the RLE structures are attributed to multiphoton resonance with laser-dressed excited states, analogous to the Freeman resonances at low intensities [23].

The further theoretical researches based on the Strong Field Approximation (SFA) obtain similar enhanced structures without considering any additional excited states [24–31]. The explanations of SFA argue that the kinetic energy of an ejected electron in ATI is $\varepsilon_n = n\omega - I_p - U_p$, where I_p is the ionization potential. Hence, when $m\omega = I_p + U_p$, there are many electrons released with near-zero kinetic energies that will be driven by the multi-cycle laser field into recollisions with the parent ion many times, and the constructive interference of a multitude of trajectories will result in the RLEs.

The semiclassical interpretations based on SFA grasp the main features that RLEs result from the constructive interference of rescattering trajectories. However, although SFA can give similar enhanced structures, the location and amplitude of the enhanced structures are far different from those of TDSE. Additionally, Kopold *et al* [26] have shown that SFA can only get a partial qualitative result compared with the experiment.

Therefore, to better understand RLEs and clarify the contribution of excited and continuum states to RLEs, in this letter a new full quantum model is established from TDSE without any excited states. The theoretical calculations of this model agree well with the results of TDSE.

Because excited states are excluded from the new model, the results confirm the arguments of SFA that the contributions of excited states to RLEs can be ignored. Further calculations show that RLEs are due to the constructive interference of different momentum transfer channels caused by the combination of the laser field and the ionic potential. For the features of multi-channel interference, the Fano-like lineshapes are also discussed in the end.

Let us start with the time-dependent Schrödinger equation in the single active electron approximation. The Hamiltonian of the electron can be expressed as

$$\begin{aligned} H(t) &= -\frac{1}{2} \frac{\partial^2}{\partial x^2} + V(x) + W(x, t) \\ &= H_a + W(x, t) = H_V + V(x), \end{aligned} \quad (1)$$

where $V(x) = -1/\sqrt{x^2 + a^2}$ represents the soft-core electron-nucleus interaction, with the soft-core parameter is chosen as $a^2 = 0.484$ to match the first ionization energy of the helium atom. $W(x, t) = xE(t)$ denotes the atom-field interaction, while H_a and H_V stand for the atomic Hamiltonian and the Hamiltonian of a free electron in an external field, respectively.

The wave functions of bound states (i.e., the functions whose corresponding eigenvalues are negative among the eigenfunctions of H_a) and the Volkov functions $\psi_p(x, t) = (2\pi)^{-1/2} \exp\{i[p + A(t)]x - i \int_0^t [p + A(\tau)]^2/2d\tau\}$ can be used to construct an overcomplete basis of the Hilbert space. Then, any wave function can be expanded by the basis functions combining the bound states and Volkov functions $\psi_p(x, t)$, i.e.,

$$\Phi(x, t) = \sum_n c_n(t) \varphi_n(x, t) + \sum_p a_p(t) \psi_p(x, t), \quad (2)$$

in which $\varphi_n(x, t) = \varphi_n(x) e^{-iE_n t}$, while $\varphi_n(x)$ is the wave function of n -th bound state of H_a and E_n is the corresponding eigenenergy. Here we should keep in mind that the Volkov states are not orthogonal to the bound states.

Substituting the expansion (2) into the Schrödinger equation, we can get

$$\begin{aligned} i \frac{\partial}{\partial t} a_q(t) &= \sum_p a_p(t) \left(V_{qp} - \sum_n \Lambda_{qn} V_{np} \right) \\ &+ \sum_m c_m(t) \left(W_{qm} - \sum_n \Lambda_{qn} W_{nm} \right), \end{aligned} \quad (3)$$

$$i \frac{\partial}{\partial t} c_m(t) = \sum_p a_p(t) V_{mp} + \sum_n c_n(t) W_{mn}, \quad (4)$$

where the matrix elements of the Coulomb interaction are $V_{qp} = \int \psi_q^\dagger(x, t) V(x) \psi_p(x, t) dx$ and $V_{np} = \int \varphi_n^\dagger(x, t) V(x) \psi_p(x, t) dx$, the matrix elements of atom-field interaction are $W_{qn} = \int \psi_q^\dagger(x, t) W(x, t) \varphi_n(x, t) dx$ and $W_{nm} = \int \varphi_n^\dagger(x, t) W(x, t) \varphi_m(x, t) dx$. Additionally, the term $\Lambda_{qn} = \int \psi_q^\dagger(x, t) \varphi_n(x, t) dx$ is caused by the fact

that the Volkov states and the bound states are not orthogonal to each other due to the features of overcomplete basis.

Furthermore, we assume that all the excited states are negligible. On the other hand, the infinite summation of momentum should be truncated in practice. Then equations (3) and (4) are changed into

$$i \frac{\partial}{\partial t} a_q(t) = \sum_p a_p(t) V_{qp}^* + c_g(t) W_{qg}, \quad (5)$$

$$i \frac{\partial}{\partial t} c_g(t) = \sum_p a_p(t) V_{gp}^*, \quad (6)$$

where $V_{qp}^* = V_{qp} f(p, t) - \Lambda_{qg} V_{gp} g(p, t)$ and $V_{gp}^* = V_{gp} g(p, t)$. The truncation functions $f(p, t)$ and $g(p, t)$ are chosen as

$$f(p, t) = \begin{cases} 1, & \text{if } [p + A(t)]^2 \leq 2B \ [B = 3.17U_p], \\ \exp[-a(|p + A(t)| - \sqrt{2B})^2], & \text{otherwise,} \end{cases} \quad (7)$$

$$g(p, t) = \begin{cases} 1, & \text{if } [p + A(t)]^2 \leq C \ [C = \min(I_p, 2U_p)], \\ \exp[-a(|p + A(t)| - \sqrt{C})^2], & \text{otherwise,} \end{cases} \quad (8)$$

where we set the dumping rate of the truncation functions $a = 5$. In the above, the truncation function $f(p, t)$ of the returned electron is set by a physical consideration that the maximum energy of the returned electron is $3.17U_p$, and the truncation energy of $g(p, t)$ is set empirically by comparing with the simulations of TDSE. Consequently, we have derived a full quantum model (Eqs. (5) and (6)) from TDSE without any excited states.

In our calculations, we use 800nm laser pulses with a total duration of 16 optical cycles, switched on and off linearly over 2 cycles. In order to observe the RLEs, we scan the laser intensity from 1.5 to $2.5 \times 10^{14} \text{W/cm}^2$. We plot the energy spectra of He atom in Fig. 1 with only the regions of plateau are considered. The results obtained by solving TDSE and our model (Eqs. (5) and (6)) are plotted in Figs. 1(a) and 1(b), respectively. Both of them show the evident resonance-like enhancements in ATI spectra. In Figs. 1(c) and 1(d), we enlarge the results of TDSE and the new model in the energy range of $2.4 \sim 3.6$ a.u., respectively, where ATI structures $\varepsilon_n = n\omega - I_p - U_p$ are visible.

Comparing the results of the two methods, one can find that the new model can reproduce the TDSE results of almost the whole regions very well in terms of structure and amplitude except for the overestimated amplitudes at laser intensities around $2.25, 2.4$ and $2.5 \times 10^{14} \text{W/cm}^2$. The new model only contains the ground and continuum states without any additional excited states. Therefore, the agreement between TDSE and the model indicates that the excited states have little effects on the structure of the resonance-like enhancements.

The regions of enhancements are irregularly located around some intensities for different energy areas. The

probability of emitted electrons at resonance regions increases from time to time with increasing intensity, exhibiting a sensitive dependence on the laser intensity. One can see that the enhanced regions are not always related to the parameter $(I_p + U_p)/\omega$, predicted by SFA [28].

In order to clarify the mechanics of RLEs, we analyze the model (Eqs. (5) and (6)). We show all three processes of the model in Fig. 2. The first process is described by W_{pg} , the direct ionization process from the ground state. Another is V_{qp}^* , the transfer process between continuum states. The third is V_{gp}^* , the recombination of the electron from the continuum state into the ground state. We can see that there are two kinds of pathways to finally occupy the continuum state with momentum p for an electron: i) direct ionization pathway described by the term W_{pg} , ii) transferring from different momenta described by the term V_{qp}^* .

It is generally believed that the ground state has little effect on the plateau of photoelectron energy spectra. Hence, in the following calculation, we set $c_g(t) = 1$, then we have

$$i \frac{\partial}{\partial t} a_q(t) = \sum_p a_p(t) V_{qp}^* + W_{qg}. \quad (9)$$

To further explore the influence of the laser field on which process plays the most important role in RLEs, we separately fix the laser peak intensities of one of the two pathways, namely the transfer process V_{qp}^* and direct ioniza-

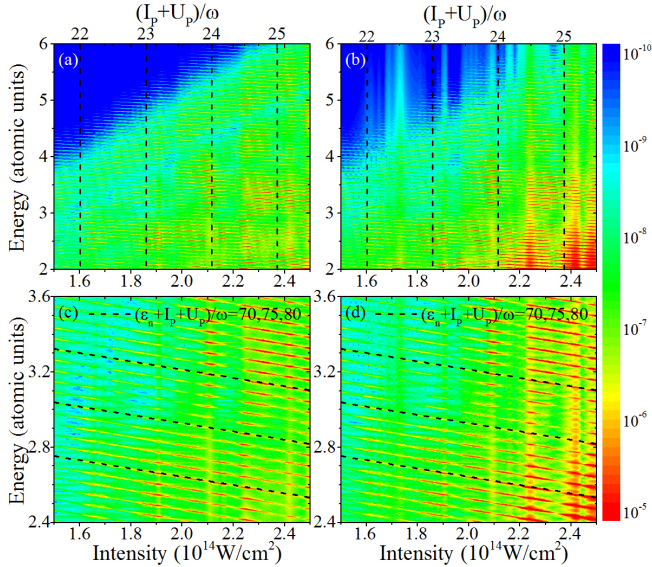


FIG. 1: Photoelectron energy spectra calculated by (a) TDSE and (b) the model, as a function of the laser intensity or the parameter $(I_p + U_p)/\omega$. Enlargement of the energy region of 2.4 ~ 3.6 a.u. for (a) and (b) are plotted in (c) and (d), respectively, where dashed lines represent the structures of ATI peaks.

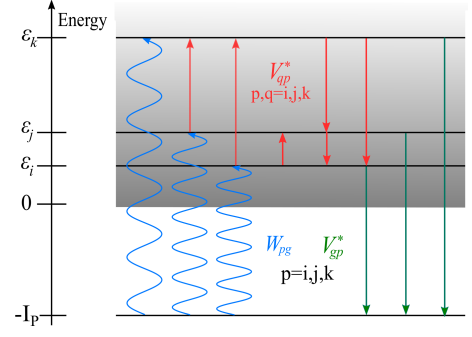


FIG. 2: Ionization diagram from the perspective of energy level transitions. $V_{qp}^*(p, q = i, j, k)$ represents that the electrons are scattered between the continuum states by Coulomb interaction, where p, k, q label three different continuum states. W_{pg} describes the transition of electrons from the ground state to different continuum states, while V_{gp}^* depicts that the electrons are recombined with the parent ion.

tion process W_{pg} , and investigate the intensity-dependent effect of the other.

At first, we keep the laser intensity of V_{qp}^* at $2 \times 10^{14} \text{ W/cm}^2$ and scan the intensity of W_{pg} from 1.5 to $2.5 \times 10^{14} \text{ W/cm}^2$. The results are plotted in Fig. 3(a), it's clearly seen that the enhanced structures disappear in the corresponding energy spectra. On the contrary, in Fig. 3(b), we fix the laser intensity of W_{pg} to $2 \times 10^{14} \text{ W/cm}^2$ and scan the intensity of the transfer process from 1.5 to $2.5 \times 10^{14} \text{ W/cm}^2$. One can see from Fig. 3(b) that the resonance pattern appears again.

The above simulations indicate that the effect of laser intensity on the momentum transfer process is of great importance to the enhanced structures. Obviously, the phase change in the momentum transfer process for different intensities has a decisive role in the enhanced structures, whereas the momentum distributions of direct ionization only change some amplitudes. Therefore, we know from Fig. 3 that the enhanced structures are caused by the sensitive dependence of the phase evolution on the laser intensity during the momentum transfer

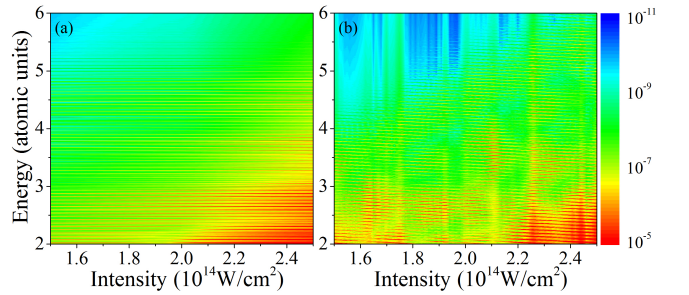


FIG. 3: Photoelectron energy spectra calculated by numerically solving Eq. (9) as a function of the laser intensity with (a) the intensity of V_{qp}^* is kept as $2 \times 10^{14} \text{ W/cm}^2$, and (b) the intensity of W_{pg} is kept as $2 \times 10^{14} \text{ W/cm}^2$.

process.

Now, we can know the resonance enhancement in the ATI spectrum is mainly due to the interference of momentum transfer processes. Different momenta may transfer to the same final momentum, and each transfer channel has a different phase. As the intensity increases, the phase changes accordingly. For some intensities, the constructive interferences occur and lead to the RLEs.

As we know, such multi-channel interference resonance may have the Fano resonance shape, and its lineshape can be fitted by the Fano formula [32]

$$R(E) = \frac{[2(E_0 - E)/\gamma + q]^2}{[2(E_0 - E)/\gamma]^2 + 1}, \quad (10)$$

where q is the Fano asymmetry parameter, E_0 is the laser intensity, E is the resonance position, and γ is the resonance width.

In order to show this property, we investigate the enhanced effects of ATI peaks which had been shown in Fig. 1. We present the differential ionization rate of different ATI peaks as a function of the laser intensity in Fig. 4(a), where the rate represents the summation of the probability of energy range from $\varepsilon_n - \omega/2$ to $\varepsilon_n + \omega/2$. The solid lines of Fig. 4(a) present the case of Fig. 1(b), and the dashed lines present the case of Fig. 3(b) where the laser intensities of the direct ionization are fixed. Comparing them, one can see that the oscillating structures varying with the intensity are very similar. The difference in amplitudes just reveals that direct ionization plays a key role in the ionization rate. For scanned intensities less than the fixed intensity, the ionization rates are overestimated. When the scanned intensities are greater than the fixed intensity, the rates are sometimes underestimated and sometimes overestimated.

In the following, we care about the regions marked in Fig. 4(a), where there are well structures and the shapes are changing hardly with the photon number n of ATI peaks. We choose the well structures and normalize the rates into an interval of $[0, 1]$. And then, we use the Fano formula (10) to fit them. The fitting parameters E , γ , and q are plotted in Figs. 4(b), 4(c), and 4(d), respectively. As can be seen from Fig. 4(b), the resonance position E increases slowly with increasing photon number n and the resonance position of Fig. 3(b) in which the laser intensity of direct ionization channel is fixed is greater than that of Fig. 1(b). The resonance width in Fig. 4(c) varies slightly and concentrates between 1.5 and $3 \times 10^{12} \text{W/cm}^2$. Figure 4(d) shows that the Fano asymmetry parameter q is negative for the photon number less than 80, while q is positive for the photon number greater than 80. More importantly, the three fitting parameters varying with the photon number in the two cases are closely similar. Due to the resonance width and Fano asymmetry parameter determine the structure together, the structures of the two cases are essentially unchanged.

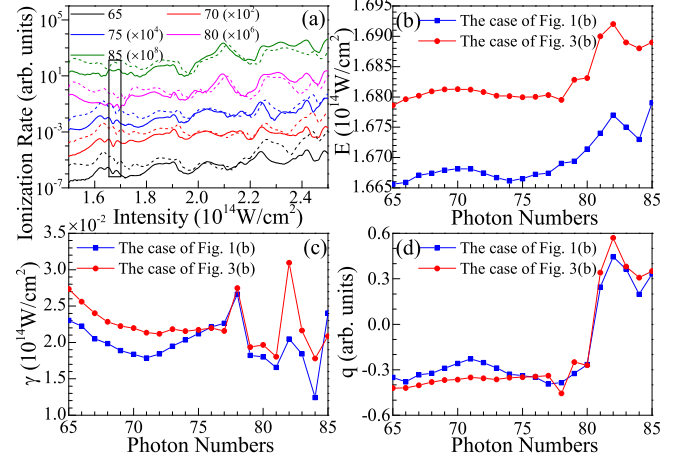


FIG. 4: (a) Differential ionization rate as a function of the laser intensity for the case of Fig. 1(b) (solid lines) and Fig. 3(b) (dashed lines) with photon numbers absorbed by electrons $n = 65, 70, 75, 80, 85$, where the results of different n are multiplied by different multiples to facilitate separation. The fitting parameters (b) E , (c) γ , and (d) q as a function of photon numbers.

Hence, by using the Fano formula, we know that the direct ionization has a small offset to the overall structure, while the shape of the enhanced structure is essentially unchanged. This also indicates that the enhanced structures are mainly due to the interference of continuum states rather than the momentum distributions of direct ionization.

In summary, we have derived a new quantum model without involving any excited states from TDSE. The calculated photoelectron energy spectra are in good agreement with the results of TDSE, indicating that the excited states are not the key to the concerned RLEs in the high-order ATI of atoms. On the contrary, the RLEs result from the constructive interference of different momentum transfer channels, while the momentum distributions of direct ionization only change some amplitudes. Finally, the Fano-like lineshapes are studied to confirm the contributions of the transfer process and the direct ionization process again. The quantum model provides a new way to investigate the quantum effects of high-order ATI, and it shed light on further understanding the related processes, such as high-order harmonic generation and nonsequential double ionization, due to their mechanisms have much in common.

This work was supported by National Natural Science Foundation of China (Grant No. 11725417, 11575027), NSAF (Grant No. U1730449), and Science Challenge Project (Grant No. 2018005).

-
- * Electronic address: lbfu@gscaep.ac.cn
- [1] W. Becker, X. J. Liu, P. J. Ho, and J. H. Eberly, *Rev. Mod. Phys.* **84**, 1011 (2012).
 - [2] R. Pazourek, S. Nagele, and J. Burgdörfer, *Rev. Mod. Phys.* **87**, 765 (2015).
 - [3] L. Y. Peng, W. C. Jiang, J. W. Geng, W. H. Xiong, and Q. H. Gong, *Phys. Rep.* **575**, 1 (2015).
 - [4] P. Agostini, F. Fabre, G. Mainfray, G. Petite, and N. K. Rahman, *Phys. Rev. Lett.* **42**, 1127 (1979).
 - [5] G. G. Paulus, W. Becker, W. Nicklich, and H. Walther, *J. Phys. B* **27**, L703 (1994).
 - [6] G. G. Paulus, W. Nicklich, H. Xu, P. Lambropoulos, and H. Walther, *Phys. Rev. Lett.* **72**, 2851 (1994).
 - [7] W. Becker, F. Grasbon, R. Kopold, D. B. Milošević, G. G. Paulus, and H. Walther, *Adv. At. Mol. Opt. Phys.* **48**, 35 (2002).
 - [8] P. B. Corkum, *Phys. Rev. Lett.* **71**, 1994 (1993).
 - [9] P. Hansch, M. A. Walker, and L. D. Van Woerkom, *Phys. Rev. A* **55**, R2535 (1997).
 - [10] M. P. Hertlein, P. H. Bucksbaum, and H. G. Muller, *J. Phys. B* **30**, L197 (1997).
 - [11] F. Grasbon, G. G. Paulus, H. Walther, P. Villorresi, G. Sansone, S. Stagira, M. Nisoli, and S. De Silvestri, *Phys. Rev. Lett.* **91**, 173003 (2003).
 - [12] C. Cornaggia, *Phys. Rev. A* **82**, 053410 (2010).
 - [13] W. Quan, X. Y. Lai, Y. J. Chen, C. L. Wang, Z. L. Hu, X. J. Liu, X. L. Hao, J. Chen, E. Hasović, M. Busuladžić, W. Becker, and D. B. Milošević, *Phys. Rev. A* **88**, 021401(R) (2013).
 - [14] C. Wang, Y. Tian, S. Luo, W. G. Roeterdink, Y. Yang, D. Ding, M. Okunishi, G. Prümper, K. Shimada, K. Ueda, and R. Zhu, *Phys. Rev. A* **90**, 023405 (2014).
 - [15] C. Wang, M. Okunishi, X. Hao, Y. Ito, J. Chen, Y. Yang, R. R. Lucchese, M. Zhang, B. Yan, W. D. Li, D. Ding, and K. Ueda, *Phys. Rev. A* **93**, 043422 (2016).
 - [16] M. J. Nandor, M. A. Walker, and L. D. Van Woerkom, and H. G. Muller, *Phys. Rev. A* **60**, R1771 (1999).
 - [17] H. G. Muller and F. C. Kooiman, *Phys. Rev. Lett.* **81**, 1207 (1998).
 - [18] H. G. Muller, *Phys. Rev. A* **60**, 1341 (1999).
 - [19] J. Wassaf, V. Vénard, R. Taïeb, and A. Maquet, *Phys. Rev. A* **67**, 053405 (2003).
 - [20] J. Wassaf, V. Vénard, R. Taïeb, and A. Maquet, *Phys. Rev. Lett.* **90**, 013003 (2003).
 - [21] R. M. Potvliege and S. Vučić, *Phys. Rev. A* **74**, 023412 (2006).
 - [22] R. M. Potvliege and S. Vučić, *J. Phys. B* **42**, 055603 (2009).
 - [23] R. R. Freeman, P. H. Bucksbaum, H. Milchberg, S. Darack, D. Schumacher, and M. E. Geusic, *Phys. Rev. Lett.* **59**, 1092 (1987).
 - [24] R. Kopold and W. Becker, *J. Phys. B* **32**, L419 (1999).
 - [25] G. G. Paulus, F. Grasbon, H. Walther, R. Kopold, and W. Becker, *Phys. Rev. A* **64**, 021401(R) (2001).
 - [26] R. Kopold, W. Becker, M. Kleber, and G. G. Paulus, *J. Phys. B* **35**, 217 (2002).
 - [27] S. V. Popruzhenko, Ph. A. Korneev, S. P. Goreslavski, and W. Becker, *Phys. Rev. Lett.* **89**, 023001 (2002).
 - [28] D. B. Milošević, E. Hasović, M. Busuladžić, A. Gazibegović-Busuladžić, and W. Becker, *Phys. Rev. A* **76**, 053410 (2007).
 - [29] D. B. Milošević, E. Hasović, S. Odžak, M. Busuladžić, A. Gazibegović-Busuladžić, and W. Becker, *J. Mod. Opt.* **55**, 2653 (2008).
 - [30] D. B. Milošević, W. Becker, M. Okunishi, G. Prümper, K. Shimada and K. Ueda, *J. Phys. B* **43**, 015401 (2010).
 - [31] X. Y. Lai, C. L. Wang, Y. J. Chen, Z. L. Hu, W. Quan, X. J. Liu, J. Chen, Y. Cheng, Z. Z. Xu, and W. Becker, *Phys. Rev. Lett.* **110**, 043002 (2013).
 - [32] U. Fano, *Phys. Rev.* **124**, 1866 (1961).